Polymer 50 (2009) 5933–5939

Contents lists available at ScienceDirect

Polymer

journal homepage: www.elsevier.com/locate/polymer

Single-molecular hybrid nano-cylinders: Attaching polyhedral oligomeric silsesquioxane covalently to poly(glycidyl methacrylate) cylindrical brushes

Youyong Xu, Jiayin Yuan, Axel H.E. Müller*

Makromolekulare Chemie II and Bayreuther Zentrum für Kolloide und Grenzflächen, Universität Bayreuth, D-95440 Bayreuth, Germany

ARTICLE INFO

Article history:
Received 20 August 2009
Received in revised form
7 October 2009
Accepted 9 October 2009
Available online 25 October 2009

Keywords:
Poly(glycidyl methacrylate)
Cylindrical polymer brush
POSS

ABSTRACT

We present the preparation of novel single-molecular hybrid nano-cylinders by covalently attaching a monothiol-functionalized polyhedral silsesquioxane (POSS-SH) to poly(glycidyl methacrylate) (PGMA) cylindrical brushes. Grafting of GMA from a long poly-initiator poly(2-(2-bromoisobutyryloxy)ethyl methacrylate) (PBIEM) via ATRP was first carried out. Gel permeation chromatography (GPC), ^{1}H NMR, dynamic light scattering (DLS), static light scattering (SLS) and atomic force microscopy (AFM) measurements confirmed the well-defined worm-like structures of the PGMA brushes. Then POSS-SH was covalently linked to PGMA brushes by reaction with about 19% of the epoxy groups. The successful preparation of the PGMA–POSS hybrid brush was demonstrated by Fourier-transform infrared spectroscopy (FTIR), DLS, SLS, energy dispersive X-ray spectroscopy (EDX) and thermogravimetric analysis (TGA) measurements. An increase of the length and diameter of the brushes was shown by AFM and non-stained transmission microscopy (TEM) measurements. Residual SiO_2 after pyrolysis of the PGMA–POSS hybrid brush in air displayed interesting cylindrical network structures.

1. Introduction

With the rapid development of nanotechnologies, a large number of materials with different functionalities on the nano-scale have been fabricated [1]. Combining inorganic materials' outstanding mechanical, optical, electric and magnetic properties, with the soft organic materials' excellent processabilities, functionalities and biocompatibilities, nano-composite materials have demonstrated their advanced performance. Their properties exceed the simple addition of each components characteristics, due to the special surface and quantum effects on the nano-scale. Polymer-based nano-composites have been widely investigated and a large category of inorganic materials, such as carbon materials, ceramics, clays, metals, metal oxides and silica, have been incorporated into different polymeric materials [2]. One advantage of these composites is that a very small amount of the added inorganic nano-materials can remarkably improve the mechanical, thermal and other properties of the polymer matrix [3]. Two general strategies have been applied to prepare the polymer-based nano-composites with inorganic materials. The easiest way is to directly disperse the nanometer-sized inorganic materials into the polymer by mechanical blending, melting or solution treatment. Surface functionalization is sometimes necessary to improve the compatibility of the inorganic materials with the polymer matrix. Recent research revealed the size of the blending materials is a key factor for the dispersing process [4]. However, the forces between the additive and the matrix are weak due to the non-covalent blending, which leads to poor property improvements and stabilities. The other method is to prepare the nano-composites via covalent linking, either by direct polymerization of functional monomers attached with inorganic groups, or by post-polymerization reactions. Thanks to the strong covalent linking of the inorganic part to the organic polymer chains, better performance of these materials is expected.

Recent progress has been achieved in the preparation of nano-composite materials on a molecular level, which find promising micro-electronic, optic and magnetic applications. Suitable nano-structured polymer matrices are in great demand. Spherically shaped polymers like star polymers [5,6], dendrimers [7] and hyperbranched polymers [8] can meet the requirements to some extent. Recently, the interest in anisotropic polymer structures is increasing, owing to their interesting properties and potential applications. One-dimensional dendronized polymers [9] and cylindrical polymer brushes (CPBs) [10,11] are the good examples. For instance, core-shell cylindrical brushes have been used as the templates for the preparation of inorganic nanowires [12–14].

* Corresponding author. Tel.: +49 921 55 3399; fax: +49 921 55 3393.
E-mail address: axel.mueller@uni-bayreuth.de (A.H.E. Müller).

0032-3861/$ – see front matter © 2009 Elsevier Ltd. All rights reserved.
doi:10.1016/j.polymer.2009.10.029

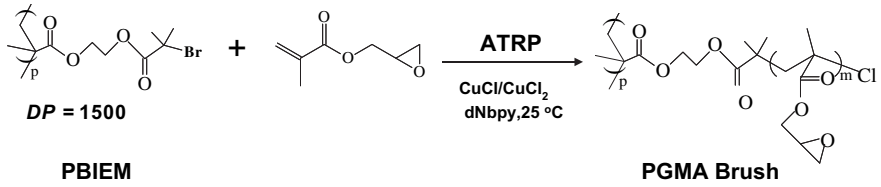

Scheme 1. Synthetic procedure for the PGMA brush.

Tedious synthetic procedures for dendronized polymers have limited their use. The relatively easier preparations of CPBs make them more attractive.

CPBs, comprised of very long backbones and densely grafted side-chains, adopt worm-like morphologies in good solvents. Their anisotropic nature causes special solution and bulk properties [15,16]. So far, grafting-to [17], grafting-through [18] and grafting-from [19,20] strategies have been explored to prepare CPBs. Generally, well-defined CPBs can be obtained by using the grafting-from method, since both the backbone and the side-chains can be grown by well-established living/controlled polymerization techniques.

In the past years, much attention has been paid to polyhedral oligomeric silsesquioxanes (POSS), which have special cage structures [21]. They are made up of silicon/oxygen $(SiO_{1.5})_n$ cages with organic substituents. Sized between 1 and 3 nm, they can be viewed as the smallest silica nanoparticles. Unlike the pure inorganic silica materials, the outside organic substituents provide them many possibilities for further functionalization, organo-compatibility, and even bio-compatibility. Incorporating POSS into polymers can dramatically improve their thermal and mechanical properties [21–24]. Different methods have been developed to prepare POSS/polymers composites. When the shell of POSS is designed to be reactive, polymers can be connected covalently to them, either by grafting-from [25] or grafting-to [26] procedures. Another convenient way is to prepare monomers carrying POSS units followed by polymerization. Controlled radical polymerizations, such as atom transfer radical polymerization (ATRP), have been successfully used to prepare homopolymers or block copolymers of POSS-containing methacrylates [27–29].

Our group has achieved single-molecular nano-composites with semi-conducting [12,13] and magnetic nanoparticles [14] non-covalently incorporated in core-shell CPBs. Very recently, we have reported the preparation of CPBs with silsesquioxanes as the core and poly[oligo(ethylene glycol) methacrylate] (POEGMA) as the water soluble shell, by consecutive ATRP of (3-acryloylpropyl)-trimethoxysilane and OEGMA and further sol–gel process [30]. They were transformed into silica nanowires by pyrolysis on a substrate.

In this work, we employed another strategy to prepare silsequioxane-containg single-molecular cylindrical nano-hybrids. By attaching thiol-functionalized POSS to the preformed poly(glycidyl methacrylate) (PGMA) cylindrical brushes, we successfully obtained nano-cylinders (termed as PGMA–POSS) which contain the cage-like inorganic materials in an organic cylindrical matrix.

2. Experimental

2.1. Materials

CuCl (97%, Aldrich) was purified by stirring with acetic acid overnight. After filtration, it was washed with ethanol and ether and then dried in vacuum oven. $CuCl_2$ (99%, Acros) was used without purification. *N*,*N*,*N*′,*N*″,*N*‴,*N*⁗-hexamethyltriethylenetetraamine (HMTETA, Aldrich) was distilled before use. 4,4′-Dinonyl-2,2′-dipyridyl (dNbpy) was purchased from Aldrich and used without further purification. Glycidyl methacrylate (GMA) (97%, Aldrich) was purified by passing through basic alumina columns before polymerization. Poly-initiator poly(2-(2-bromoisobutyryloxy)ethyl methacrylate) (PBIEM) ($DP_n = 1500$, $PDI = 1.08$) was reported previously [31]. Mercaptopropyl-isobutyl-POSS (POSS-SH) (from Aldrich, molecular weight: 892 Da) was used as it is. All the other solvents and chemicals were used as received.

2.2. Preparation of PGMA brushes onto PBIEM

The grafting of GMA was carried out in a round-bottom flask sealed with a rubber septum. PBIEM (55.8 mg, 0.2 mmol of

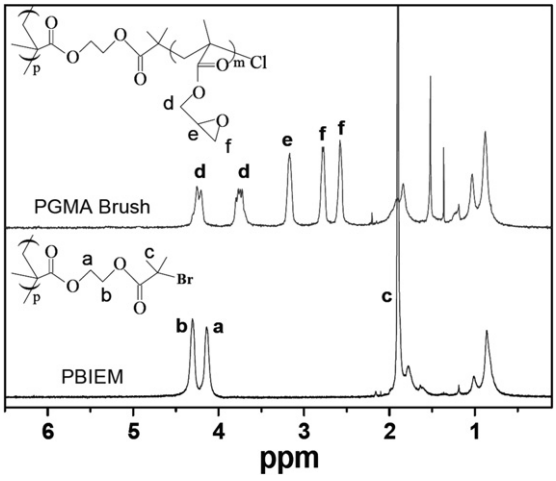

Fig. 1. ^{1}H NMR spectra of PBIEM and PGMA brush in $CDCl_3$.

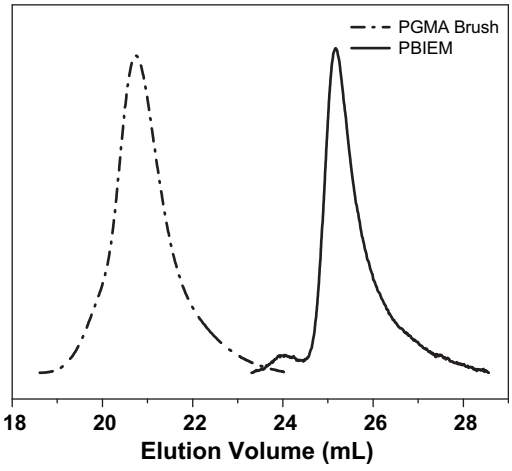

Fig. 2. GPC elution curves of PBIEM poly-initiator and the PGMA brush in THF.

Table 1
Molecular characterization of brushes.

Sample	Conv.[a]	$DP_{sc,calc}$[b]	$10^7 \times M_{n,calc}$[c]	$10^7 \times M_{w,SLS}$[d]	R_g,[e] nm	$R_{h,app}$,[f] nm (*PDI*)	R_g/R_h
PGMA brush	24.9%	125	2.70	3.26	104	57 (0.24)	1.82
PGMA–POSS	N/A	N/A	N/A	8.12	112	62 (0.17)	1.81

[a] Monomer conversion determined by ^{1}H NMR.
[b] Calculated *DP* of side-chains, $DP_{sc,calc} = ([M]_0/[I]_0) \times$ conversion.
[c] Calculated from monomer conversion. $M_{n,calc}$ = (monomer molecular weight $\times DP_{sc,calc} + 234.5) \times DP_{backbone}$.
[d] Determined by SLS in dioxane or THF solutions for PGMA and PGMA–POSS, respectively.
[e] Radii of gyration measured by SLS.
[f] Apparent hydrodynamic radii and polydispersities measured by DLS in dioxane or THF solutions for PGMA and PGMA–POSS, respectively.

initiating α-bromoester groups) and 4,4′-Dinonyl-2,2′-dipyridyl (dNbpy) (163.5 mg, 0.4 mmol) were dissolved in anisole (28 g) in a pear-shaped flask and stirred overnight to assure the complete dissolution of the high molecular weight poly-initiator. Then the monomer GMA (14.2 g, 0.1 mol) was injected via a syringe and stirred for 15 min. The flask was purged with argon for 15 min. About 0.5 mL of solution was taken out with an argon-purged syringe as an initial sample for conversion measurement by ^{1}H NMR. A round-bottom flask with CuCl (20 mg, 0.2 mmol) and $CuCl_2$ (1.4 mg, 0.01 mmol) was also deoxygenated by argon flow. Then the solution in the pear-shaped flask was transferred into the round-bottom flask by a cannula. The solution immediately turned brown. The round-bottom flask was then inserted into a water-bath at 25 °C. Small amount of samples were taken out at intervals to check the monomer conversion. After 32 h, the conversion determined by ^{1}H NMR reached 24.9%. The round-bottom flask was then opened to air. THF was added to dilute the solution and the color of the solution turned green. After passing through a basic alumina column, it was precipitated into cold hexane. Then it was re-dissolved in dioxane. White powders were obtained after freeze-drying.

2.3. Preparation of PGMA–POSS hybrid brushes

The PGMA brush was dissolved in THF in a bottle and POSS-SH was added (2-fold to the glycidyl groups in PGMA), followed by vigorous stirring. Then small amount of pyridine was added to the solution. It was subjected to heating at 65 °C. The reaction was kept for 7 days. Afterwards, it was cooled to room temperature and was purified by ultrafiltration through a membrane with the pore size of 200 nm using THF as the eluent.

2.4. Characterization

^{1}H NMR was measured on a Bruker AC-250 instrument at room temperature using $CDCl_3$ as the solvent.

Conventional *gel permeation chromatography* (GPC) using THF as eluent at a flow rate of 1.0 mL/min at room temperature was performed for the PGMA brush. Column set: 5 μm p SDV gel, 10^2, 10^3, 10^4, and 10^5 Å, 30 cm each (PSS, Mainz). Detectors used are RI and UV operated at 254 nm. Polystyrene standards (PSS, Mainz) with narrow molecular weight distribution were used for the calibration of the column set.

Fourier-transform infrared (FTIR) spectra were recorded at room temperature using a Bruker FTIR EQUINOX 55/S spectrometer at a resolution of 4 cm^{-1}. The samples were prepared by casting sample solutions onto NaCl plates.

Dynamic light scattering (DLS) was carried out on an ALV DLS/SLS-SP 5022F compact goniometer system with an ALV 5000/E correlator and a He–Ne laser ($\lambda = 632.8$ nm) at angle of 90°. Before the light scattering measurements, the sample solutions were filtered 3 times by using Millipore Teflon filters. CONTIN analyses were taken for the measured intensity correlation functions. Apparent hydrodynamic radii, R_h, of the brushes were calculated according to the Stokes–Einstein equation. All the measurements were carried out at 25 °C.

Static light scattering (SLS) was measured on a Sofica goniometer using a He–Ne laser ($\lambda = 632.8$ nm). Prior to the light scattering measurements, the sample solutions were filtered 3 times. Five concentrations of the brush solutions were measured at angles in the range from 30° to 150°. Absolute weight-average molecular weights, M_w, and radii of gyration, R_g, were obtained by the analysis of the Zimm-plots. The refractive index increments of the PGMA brush in dioxane and PGMA–POSS in THF at 25 °C were measured to be $dn/dc = 0.07361$ mL/g and 0.08092 mL/g, respectively, using a PSS DnDc-2010/620 differential refractometer.

Atomic force microscopy (AFM) measurement in liquid was carried out on a Digital Instruments Nanoscope Multimode using anisole as the solvent. The measurements were performed at room temperature. AFM measurement of dry PGMA–POSS was performed on a Digital Instruments Dimension 3100 microscope operated in tapping mode. The micro-cantilever used for the AFM measurements were from Olympus with resonant frequencies between 284.3 kHz and 386.0 kHz, and spring constants ranging from 35.9 to 92.0 N/m. Carbon-coated mica substrates were prepared using a Balzers MED 010 mini-deposition system. Carbon with a thickness of approximately 10 nm was deposited on the freshly cleaved mica surfaces by evaporation. The samples were

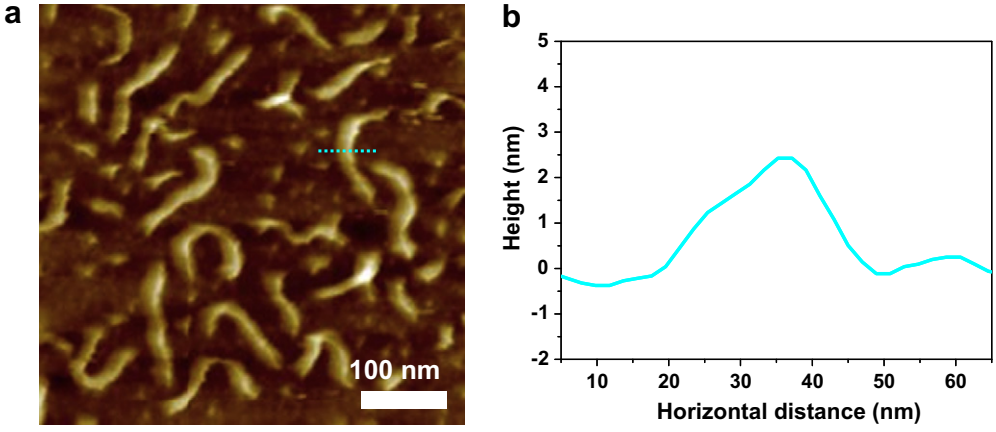

Fig. 3. (a) AFM height image of the PGMA brush on mica in anisole, Z range 7 nm; and (b) section analysis of the cursor shown in (a).

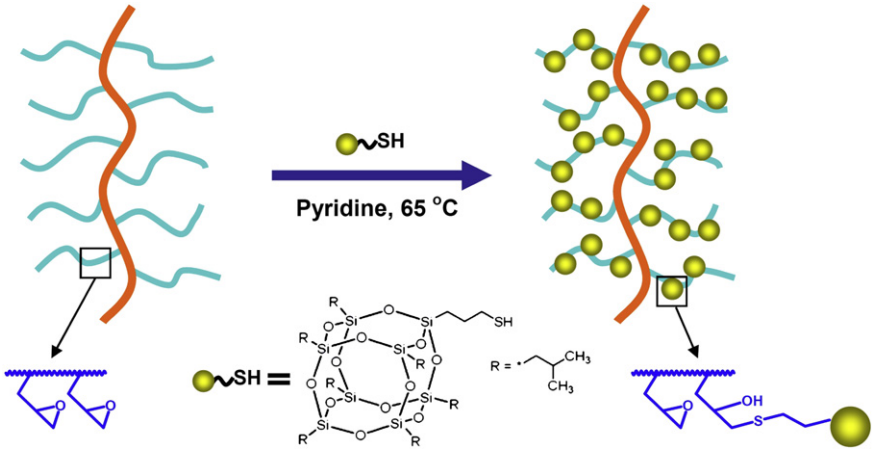

Scheme 2. Procedure for the preparation of nano-hybrid PGMA–POSS brush.

prepared by dip-coating from very dilute (0.01 g/L) THF solution of PGMA–POSS onto carbon-coated mica surface.

Scanning electron microscopy (SEM) and energy dispersive X-ray spectroscopy (EDX) were measured on a Zeiss, LEO 1530 FESEM.

Non-stained *transmission electron microscopy* (TEM) measurements were performed on a LEO 922 OMEGA, operated at 200 kV.

Thermogravimetric analyses (TGA) were performed on Netzsch 409 °C, in air atmosphere, with the temperature ranging from 25 °C to 65 °C and heat rate of 10 K/min.

3. Results and discussion

3.1. Synthesis of the PGMA brush

To prepare the hybrid PGMA–POSS brushes, precursor CPBs with poly(glycidyl methacrylate) (PGMA) side-chains were first synthesized by grafting from a narrowly distributed poly-initiator PBIEM ($M_n = 4.18 \times 10^5$, $DP_n = 1500$, $PDI = 1.08$) [31] using ATRP. Scheme 1 depicts the synthetic process.

It has been known that the initiating efficiency for the grafting of bulky monomers, e.g. methacrylates, by ATRP is well below 100% [32,33]. Some measures were taken to improve it. CuCl/$CuCl_2$ catalysts were used instead of CuBr, to enhance the initiating process and lower the rate of propagation, utilizing the halogen exchange process [34]. In addition, the concentration of monomer was kept very low (around 30 wt%). Preliminary polymerizations using HMTETA as the ligand led to insoluble materials, suggesting the polymerization was too fast. So, the weaker ligand 4,4′-Dinonyl-2,2′-dipyridyl (dNbpy) was used to decelerate the polymerization. Due to the existence of very reactive epoxy groups in the monomer, the polymerization was carried out at room temperature to avoid possible side-reactions at high temperatures.

Fig. 1 shows the ^{1}H NMR spectra of poly-initiator PBIEM and the as-prepared PGMA brush. The peaks from the PBIEM (methylene groups linking the ester groups at 4.1 ppm and 4.3 ppm; and methyl groups neighboring bromide groups at 1.9 ppm) become much less distinctive, and the specific peaks for PGMA (methylene group linking the ester bond and epoxy, at 3.7 ppm and 4.2 ppm; and hydrogens in the epoxy ring, at 2.6 ppm, 2.8 ppm and 3.2 ppm) rise significantly. This indicates the success of the grafting reaction.

GPC measurements were performed for the comparison of PBIEM and PGMA. Although they cannot provide the true molecular weights and polydispersities of CPBs, the elution curves can be used to reflect the shift of the molecular weights. Fig. 2 displays the GPC

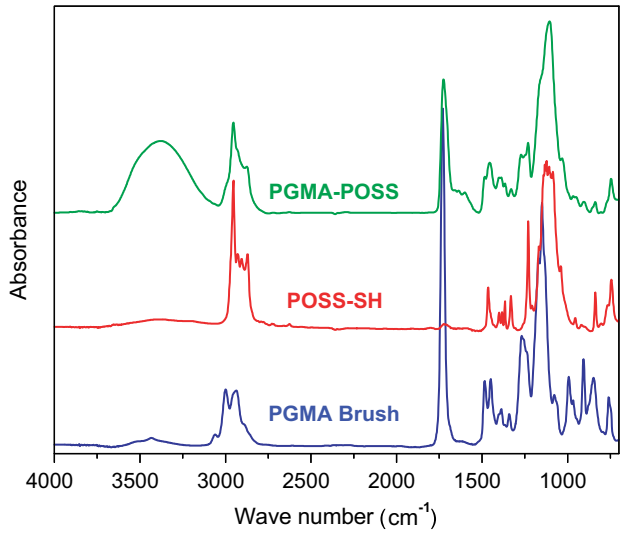

Fig. 4. FTIR spectra of PGMA brush, POSS-SH and PGMA–POSS on NaCl.

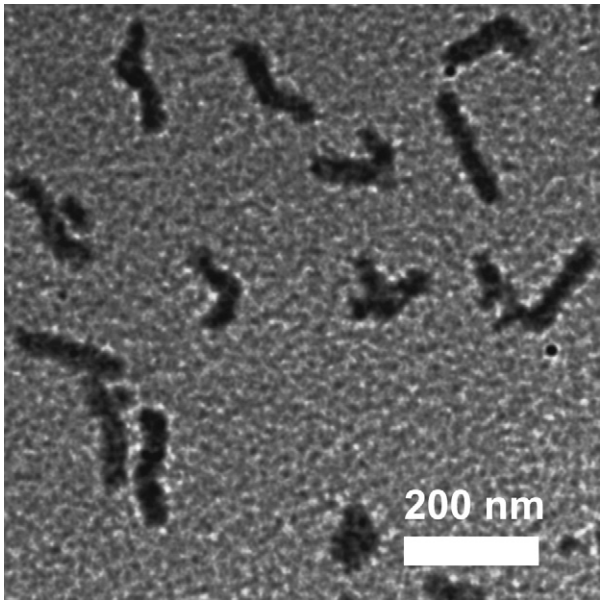

Fig. 5. Non-stained TEM image of PGMA–POSS hybrid brushes on a carbon-coated TEM grid.

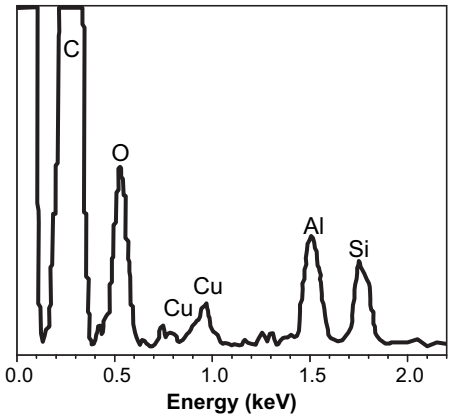

Fig. 6. EDX spectrum of PGMA–POSS on a carbon-coated TEM grid.

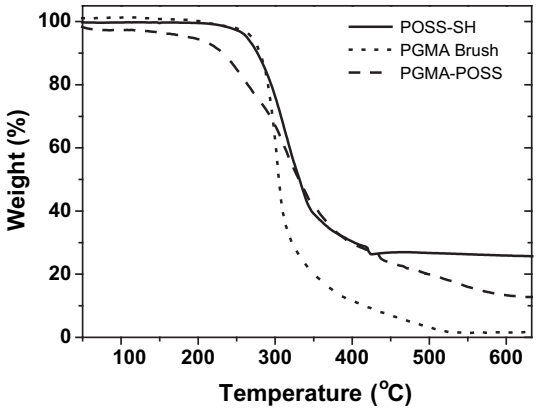

Fig. 8. TGA measurements of PGMA brush, POSS-SH and PGMA–POSS in air.

elution curves of PBIEM and PGMA. A small shoulder peak for PBIEM has been reported before [31], which does not influence the preparation of CPBs, due to the very low fraction in the whole polymer. It can be clearly seen that the mono-modal peak for the PGMA brush was shifted in the direction of higher molecular weight. There is almost no intersection for the two peaks, which suggests the successful grafting-to the poly-initiator.

PGMA brush solutions in dioxane were subjected to SLS and DLS measurements to obtain the true molecular weight and size. Table 1 (first entry) lists the results. The calculated number-average molecular weight, $M_{n,\mathrm{calc}}$, is comparable to the weight-average molecular weight, M_w, indicating the low polydispersity ($M_w/M_n = 1.21$ in this case) of the PGMA brush. So this also suggests the successful preparation of the brush. The DLS measurement shows that the apparent hydrodynamic radius of the PGMA brush in dioxane is around 57 nm, and the *PDI* is about 0.24, which is relatively low for a brush of such high molecular weight. The ratio R_g/R_h is 1.82, typical for worm-like molecules, indicating the stretching of the backbone of the brush by the very long and crowded PGMA side-chains.

Because of the epoxy groups in the monomer units, it is hard to determine the initiating efficiency of the brush by detaching the side-chains and determining their molecular weight. According to the commonly reported values for methacrylates [35,36], the initiating efficiency in this case should be in the range of $50 \pm 10\%$. So the true DP_n of the side-chains is estimated as 250 ± 50.

Due to dewetting it is not possible to measure AFM of the PGMA brush in the dry state. True morphologies of the PGMA brush were recorded by AFM in solution. Fig. 3a shows the AFM height image of the PGMA brush on mica in anisole, a good solvent for PGMA brush. Clear worm-like structures can be observed, and the average length of the brushes is about 130 nm, which is shorter than the other brushes prepared by the same poly-initiator [35,36]. The backbone is stretched to only 35% of the contour length ($l_c = 0.25$ nm $\times$ $DP = 375$ nm), due to the somewhat lower grafting density. The section analysis in Fig. 3b shows that the height of the brushes is around 2.5 nm.

These results indicate that a well-defined PGMA brush was successfully prepared by grafting the epoxy containing monomer to the long linear poly-initiator.

3.2. Preparation of the hybrid PGMA–POSS cylindrical brush

It has been reported that the highly active epoxy groups can react with mercaptans in the presence of a base [37]. Thus, by attaching a monothiol-functionalized POSS to the epoxy containing PGMA brushes, hybrid nano-cylinders were obtained. Scheme 2 shows the process for the reaction.

The as-prepared hybrid can be well dissolved in dilute THF solutions. When it was dried, it could not be dissolved again. So it is hard to perform ^{1}H NMR measurements for this material. Instead, FTIR measurements of the solution-cast samples on NaCl plates were performed. Fig. 4 shows the FTIR spectra of the POSS-SH, PGMA brush and hybrid PGMA–POSS. Almost no absorption is observed at around 3500 cm^{-1} for the precursor POSS-SH and PGMA brush, indicating absence of hydroxyl groups. In contrast, a strong and broad peak around 3500 cm^{-1} was clearly seen for the hybrid material PGMA–POSS, indicating the abundance of hydroxyl

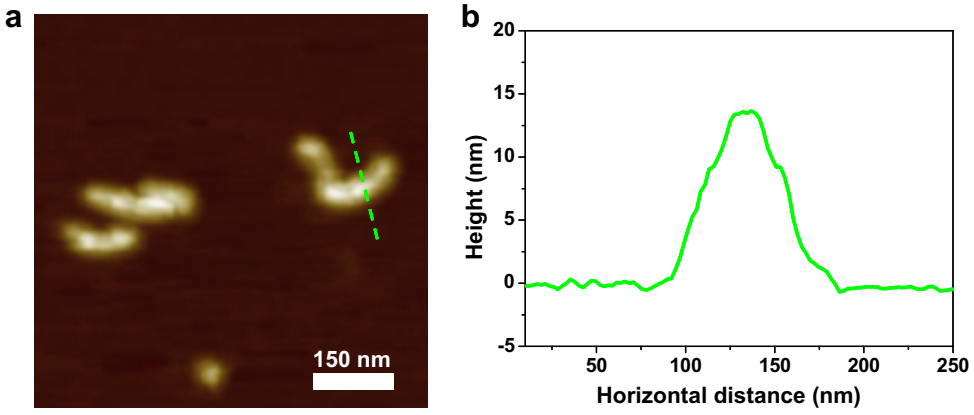

Fig. 7. (a) AFM height image of PGMA–POSS hybrid brushes on a carbon-coated mica surface, Z range 30 nm; and (b) section analysis of the cursors present in (a).

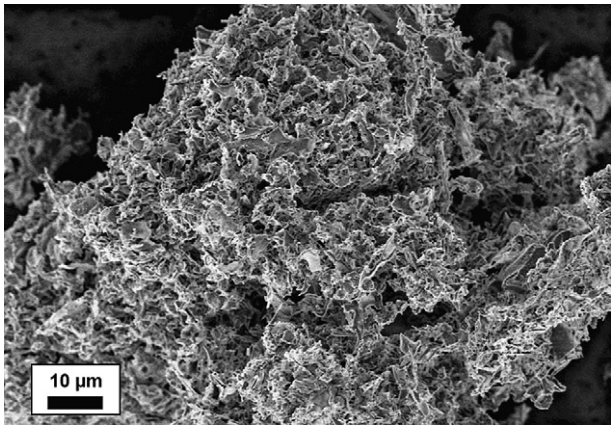

Fig. 9. SEM image of the residual SiO_2 after pyrolysis of the PGMA–POSS hybrid brush in air.

groups in this brush, as depicted in Scheme 2. The spectrum of PGMA–POSS also shows the coexistence of the strong peaks attributed to the ester groups (around 1720 cm^{-1}) from the PGMA precursor and Si-O (around 1100 cm^{-1}), demonstrating the success of the fabrication of the hybrid materials.

Light scattering measurements were also carried out for the hybrid PGMA–POSS. From the results listed in Table 1 (entry 2), we can see that M_w has been significantly increased from 3.26×10^7 to 8.12×10^7 when POSS-SH was attached to PGMA brush. A small increase of R_g and $R_{h,app}$ is also observed. According to the molecular weight values, the grafting efficiency of POSS-SH to PGMA brush is calculated to be 19.2%. The rather low attaching efficiency is due to the high steric hindrance inside the PGMA brush.

Non-stained TEM measurements were performed for both PGMA brush and PGMA–POSS brush to observe their morphologies. In the image of the PGMA brush (see Supporting information, Figure S1), no clear objects could be identified, due to the low contrast of the pure polymer brush. In contrast, in the non-stained TEM image of PGMA–POSS (Fig. 5) clear nano-cylinders can be observed and their lengths are around 150 nm, which is somewhat higher than that of precursor PGMA brushes on mica surface, likely caused by the stretching effect of the attached POSS-SH. The increase of the contrast in the TEM measurements provides another proof that the high-contrast POSS nanoparticles have been attached to the brushes.

The same sample on the carbon-coated grid for the TEM measurement was directly subjected to EDX measurement on an aluminum sample holder. In addition to the peaks for copper, aluminum and carbon from the TEM grid and sample holder, a clear peak for silicon at 1.75 keV is observed in Fig. 6. This qualitatively proves the existence of silicon, and thus POSS in the PGMA–POSS hybrid.

AFM of the PGMA–POSS hybrid brush supplied more information of the hybrid. Fig. 7 shows the AFM height image of PGMA–POSS on carbon-coated mica surface. It can be seen that the length of some brushes exceeds 150 nm, suggesting the effect of the attached POSS-SH. Further section analysis discloses that the height of these hybrid cylinders is around 14 nm, which is much higher than that of the pure PGMA in solution.

3.3. Pyrolysis of hybrid brushes

The hybrid PGMA–POSS brush was subjected to thermogravimetric analysis (TGA). Fig. 8 displays the results of the pure PGMA brush, POSS-SH, and PGMA–POSS in air. The degradation temperature for PGMA–POSS hybrid is somewhat lower than those of the precursor PGMA and POSS-SH, probably a result of the epoxy groups ring-opening and formation of large number of hydroxyl groups. After the heating process, almost nothing was left from the pure PGMA brush, while some residuals are observed for POSS-SH and PGMA–POSS. EDX analysis (see Supporting information, Figure S2) of these residuals shows the main components of the residuals are silicon and oxygen, suggesting their nature as SiO_2. For POSS-SH, the residual amount of silica is 26%, which is much less than the calculated value of 41%. This could be because considerable amount of SiO_2 dust was flushed away by the air flow in the TGA measurement. The same could have happened to the hybrid PGMA–POSS. Taking into account the measured residual silica, the efficiency of the attaching of POSS-SH would be only 9.0%. A big proportion of formed SiO_2 dust must have been brought away by the flowing air, which may have caused the discrepancy of the attaching efficiency values.

The residual SiO_2 was collected for SEM measurement, as shown in Fig. 9. Loosely distributed layers are observed. A more detailed analysis of these materials was performed by TEM. As displayed in Fig. 10a, textured structures are found on the layered structures. The enlarged image shown in Fig. 10b, however, reveals that the light dots are connected cylindrical objects. We assume that these are holes stem from the transformation of the

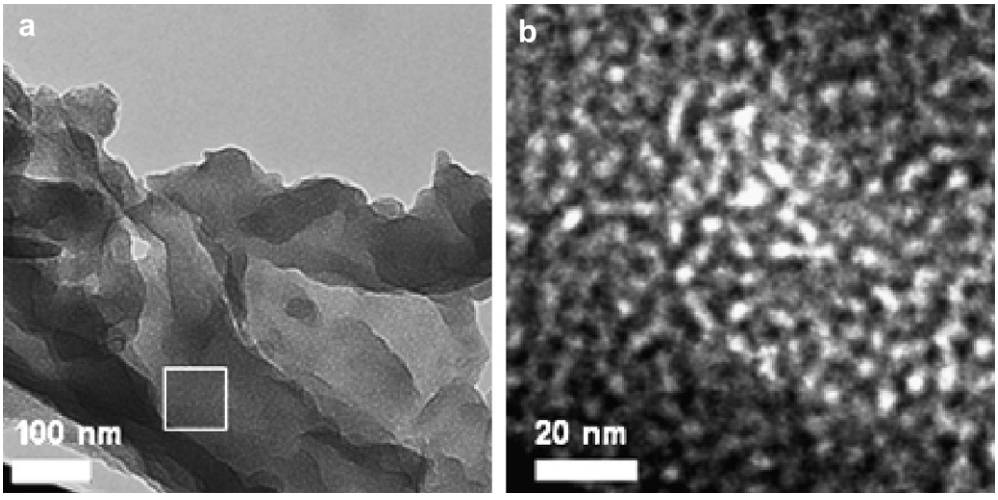

Fig. 10. TEM image of the residual SiO_2 after pyrolysis of the PGMA–POSS hybrid brush in air; (b) zoom of image (a).

cylindrical organic part of the PGMA–POSS precursor at high temperature.

4. Conclusions

We have demonstrated the successful fabrication of single-molecular nano-hybrid cylinders by attaching thiol-functionalized POSS to CPBs with poly(glycidyl methacrylate) side-chains. A PGMA brush was first prepared by grafting of GMA from a long poly-initiator PBIEM via ATRP. ^{1}H NMR, GPC, DLS, SLS and AFM measurements confirmed the well-defined worm-like structures of PGMA brushes. Then monothiol-functional POSS was covalently attached to the PGMA brushes by reaction with the epoxy groups. FTIR, DLS, SLS, EDX and TGA measurements evidenced the achievement of the hybrid PGMA–POSS brushes. Due to the steric hindrance, only 20% of the epoxy groups reacted with POSS-SH, according to SLS before and after functionalization. Both the length and the diameter of the brushes increased due to functionalization, as indicated by AFM and non-stained TEM measurements. The residual SiO_2 obtained from the pyrolysis of PGMA–POSS in TGA measurement showed interesting connected cylindrical structures.

Acknowledgements

The authors want to express their gratitude to Mr. Benjamin Gossler (BIMF, Universität Bayreuth) for the SEM and EDX measurements. Help from Christina Löffler and Sandra Ganzleben (MC I, Universität Bayreuth) with the TGA measurements is appreciated. Constructive discussions with Dr. Weian Zhang are gratefully acknowledged. We thank Deutsche Forschungsgemeinschaft (DFG) for the financial support within SPP 1165 (Nanowires and Nanotubes).

Appendix. Supporting information

Supporting information associated with this article can be found, in the online version, at doi: 10.1016/j.polymer.2009.10.029.

References

[1] Gross M. Springer handbook of nanotechnology. Berlin: Springer-Verlag; 2005.
[2] Schaefer DW, Justice RS. Macromolecules 2007;40:8501–17.
[3] Paul DR, Robeson LM. Polymer 2008;49:3187–204.
[4] Mackay ME, Tuteja A, Duxbury PM, Hawker CJ, Horn BV, Guan Z, et al. Science 2006;311:1740–3.
[5] Hadjichristidis NJ. Polym Sci Part A Polym Chem 1999;37:857–71.
[6] Hadjichristidis N, Pispas S, Pitsikalis M, Iatrou H, Vlahos C. Adv Polym Sci 1999;142:71–127.
[7] Vögtle F, Gestermann S, Hesse R, Schwierz H, Windisch B. Prog Polym Sci 2000;25:987–1041.
[8] Inoue K. Prog Polym Sci 2000;25:453–571.
[9] Schlüter AD, Rabe JP. Angew Chem Int Ed 2000;39:864–83.
[10] Zhang M, Müller AHE. Polym Sci Part A Polym Chem 2005;43:3461–81.
[11] Sheiko SS, Sumerlin BS, Matyjaszewski K. Prog Polym Sci 2008;33:759–85.
[12] Yuan J, Drechsler M, Xu Y, Zhang M, Müller AHE. Polymer 2008;49:1547–54.
[13] Zhang M, Drechsler M, Müller AHE. Chem Mater 2004;16:537–43.
[14] Zhang M, Estournes C, Bietsch W, Müller AHE. Adv Funct Mater 2004;14:871–82.
[15] Wintermantel M, Fischer K, Gerle M, Ries R, Schmidt M, Kajiwara K, et al. Angew Chem Int Ed 1995;34:1472–4.
[16] Bolisetty S, Airaud C, Xu Y, Müller AHE, Harnau L, Rosenfeldt S, et al. Phys Rev E 2007;75. 040803/040801–040803/040804.
[17] Gao H, Matyjaszewski K. J Am Chem Soc 2007;129:6633–9.
[18] Dziezok P, Sheiko SS, Fischer K, Schmidt M, Möller M. Angew Chem Int Ed 1997;36:2812–5.
[19] Beers KL, Gaynor SG, Matyjaszewski K, Sheiko SS, Möller M. Macromolecules 1998;31:9413–5.
[20] Börner HG, Beers K, Matyjaszewski K, Sheiko SS, Möller M. Macromolecules 2001;34:4375–83.
[21] Li G, Wang L, Ni H, Pittman Jr CU. J Inorg Organomet Polym 2002;11:123–54.
[22] Kannan RY, Salacinski HJ, Butler PE, Seifalian AM. Acc Chem Res 2005;38:879–84.
[23] Pielichowski K, Njuguna J, Janowski B, Pielichowski J. Adv Polym Sci 2006;201:225–96.
[24] Phillips SH, Haddad TS, Tomczak SJ. Curr Opin Solid State Mater Sci 2004;8:21–9.
[25] Ohno K, Sugiyama S, Koh K, Tsujii Y, Fukuda T, Yamahiro M, et al. Macromolecules 2004;37:8517–22.
[26] Pyun J, Matyjaszewski K. Chem Mater 2001;13:3436–48.
[27] Pyun J, Matyjaszewski K. Macromolecules 2000;33:217–20.
[28] Pyun J, Matyjaszewski K, Wu J, Kim G-M, Chun SB, Mather PT. Polymer 2003;44:2739–50.
[29] Pyun J, Matyjaszewski K, Kowalewski T, Savin D, Patterson G, Kickelbick G, et al. J Am Chem Soc 2001;123:9445–6.
[30] Yuan J, Xu Y, Walther A, Bolisetty S, Schumacher M, Schmalz H, et al. Nat Mater 2008;7:718–22.
[31] Zhang M, Breiner T, Mori H, Müller AHE. Polymer 2003;44:1449–58.
[32] Neugebauer D, Sumerlin BS, Matyjaszewski K, Goodhart B, Sheiko SS. Polymer 2004;45:8173–9.
[33] Sumerlin BS, Neugebauer D, Matyjaszewski K. Macromolecules 2005;38:702–8.
[34] Matyjaszewski K, Shipp DA, Wang J-L, Grimaud T, Patten TE. Macromolecules 1998;31:6836–40.
[35] Xu Y, Becker H, Yuan J, Burkhardt M, Zhang Y, Walther A, et al. Macromol Chem Phys 2007;208:1666–75.
[36] Xu Y, Bolisetty S, Drechsler M, Fang B, Yuan J, Ballauff M, et al. Polymer 2008;49:3957–64.
[37] Carioscia JA, Stansbury JW, Bowman CN. Polymer 2007;48:1526–32.